EUR 3563e

EUROPEAN ATOMIC ENERGY COMMUNITY - EURATOM

A COMPARISON OF THE Pu-O SYSTEM WITH THE RARE EARTH OXIDE SYSTEMS Ce-O, Pr-O AND Tb-O

by

H. BLANK

1967

Joint Nuclear Research Center
Karlsruhe Establishment - Germany

Institute of Transuranium Elements

...ued
at higher
where differences

This report is on sale at the addresses listed on cover page 4

at the price of FF 6.—	FB 60	DM 4.80	Lit. 750	Fl. 4.30

When ordering, please quote the EUR number and the ' which are indicated on the cover of each report.

This

exist between the two groups of diagrams. In this range the rare earth oxides exibit disturbed pseudo cubic intermediate phases whereas the Pu-O system does not show them. This difference in behaviour can be correlated with the change of the lattice parameters of the cubic and pseudo cubic phases with the O/M-ratio and with their dependence on temperature. It gives indications on the type of interaction between the lattice defects in these oxide systems. For the Pu-O system it is shown that a new modified phase diagram is in good agreement with published x-ray and EMF data.

EUR 3563e

EUROPEAN ATOMIC ENERGY COMMUNITY - EURATOM

A COMPARISON OF THE Pu-O SYSTEM WITH THE RARE EARTH OXIDE SYSTEMS Ce-O, Pr-O AND Tb-O

by

H. BLANK

1967

Joint Nuclear Research Center
Karlsruhe Establishment - Germany

Institute of Transuranium Elements

SUMMARY

The phase diagrams and the lattice parameters of the cubic and pseudo cubic phases of the Pu-O system on the one side are compared with those of the Ce-O, Pr-O and Tb-O systems on the other side. The features common to all four phase diagrams are an extended region MO_{2-x} above 650° C, a miscibility gap between MO_2 and $MO_{1.83}$ or $MO_{1.70}$ at low temperatures and a modified C type phase at higher temperatures for $O/M \leq 1.69$.

This leaves $1.83 = O/M = 1.71$ as the region where differences exist between the two groups of diagrams. In this range the rare earth oxides exibit disturbed pseudo cubic intermediate phases whereas the Pu-O system does not show them. This difference in behaviour can be correlated with the change of the lattice parameters of the cubic and pseudo cubic phases with the O/M-ratio and with their dependence on temperature. It gives indications on the type of interaction between the lattice defects in these oxide systems.

For the Pu-O system it is shown that a new modified phase diagram is in good agreement with published x-ray and EMF data.

KEYWORDS

PHASE DIAGRAMS
LATTICES
PLUTONIUM OXIDES
CERIUM OXIDES
TERBIUM OXIDES
PRASEODYMIUM OXIDES

C O N T E N T S

	Page
1. Introduction	4
2. The phase diagrams of the oxides of Pu, Ce, Pr and Tb	5
3. Lattice parameters of cubic and pseudo cubic phases	9
3.1. General behaviour	9
3.2. The region 2,00 = O/M = 1,83 and ist lattice parameters	9
3.3. Low oxygen boundary of the miscibility gap in the rare earth systems and some aspects of defect interaction in the region 1,83 = O/M = 1,71	14
3.4. The C'-type phase O/M 1,69	17
4. Partial free enthalpy data in the Pu-O and Ce-O systems and their relation with the phase diagrams	19
4.1. The partial molar quantities of the Ce-O and Pu-O systems	19
4.2. Comparison of partial molar free enthalphy data with the corresponding phase diagrams and lattice parameters.....	20

A COMPARISON OF THE Pu-O SYSTEM WITH THE RARE EARTH OXIDE SYSTEMS Ce-O, Pr-O AND Tb-O(+)

1. Introduction

The purpose of this paper is a comparison of the Pu-O system on the one side with the rare earth oxide systems of Ce, Pr and Tb on the other side in order to find those properties of the two groups of oxides which are in common and those which are different. By this means it is hoped to help to the understanding of the plutonium oxides, Since we are concerned principally with features to be found in both groups, we shall not go into the involved details of the disturbed fluorite structures in the rare earth oxides. The incentive to this paper were some new results on the Pu-O phase diagram found recently [7]

(+)Manuscript received on June 21, 1967.

2. The phase diagrams of the oxides of Pu,Ce,Pr and Tb

Though the phase diagrams of the oxyde systems Pu-O, Ce-O, Pr-O and Tb-O are still far from complete sufficient data exist at lower temperatures for a first attempt to compare some main features. The similarities which exist between them are based on the following mutual facts :

i) The cations can occur either tetravalent or trivalent in the oxides of these four metals depending on the oxygen partial pressure above the crystal,

ii) All tetravalent oxides have the fluorite structure,

iii) The trivalent oxides exist in the rare earth bcc C-type or in the hexagonal A-type structure depending on temperature,

iv) The cations of Pu, Ce and Pr have about the same ionic radii in the trivalent and also in the tetravalent state. Terbium makes an exception. Its ions are sensibly smaller in both states.

The four phase diagrams are shown in figures 1 to 4.

The Pu-O diagram is based on the work of [12] [17] and[7], and will be discussed in section 4.2. The Ce-O diagram is taken from the work of [2] and [3], the Pr-O diagram from an article by [13] with the inclusion of the work on the phase transition of Pr_2O_3 by [10] and the Tb-O system by [13].

Comparing the four diagrams, we find the Tb-O system somewhat out of the general trend for two reasons. The oxide TbO_2 can only be prepared with difficulty under extreme pressures of O_2 and on the other hand Tb_2O_3 does not exist in the hexagonal A form. This may be a consequence of the rather small radii of its cations. Therefore we shall exclude this system in some parts of the following discussion.

A rather close relationship between the diagrams of Pu-O, Ce-O and Pr-O, apart from the four points mentioned above, is indicated by the following properties common to all three systems :

v) An extended single phase field MO_{2-x} exists above about 650° C from MO_2 to at least down to $MO_{1,83}$ or, as in the case of Pu-O down to about $MO_{1,71}$.

vi) At temperatures below the MO_{2-x} single phase field ($T < 650°$ C) a two phase miscibility gap exists containing as the two phases MO_{2-x} ($x \approx 0,005$) and the first stable suboxide of each system. The latter is about $MO_{1,82}$ to $MO_{1,83}$ for the rare earth oxides, and $MO_{1,69}$ to $MO_{1,62}$ for the Pu-O system at 650° C $> T >$ 350° C.

vii) At $MO_{1,69}$ a high temperature bcc C type phase appears which is called C'-phase here in order to distinguish it from the true M_2O_3 C-type structure (bixbite). The C'-type phase extends from O/M = 1,69 to lower O/M ratios of varying degree depending on the oxide system. For Pu-O the lower limit is for instance O/M = 1,62. At the same temperature level towards lower oxygen contents the C'phase is followed by a two phase field A + C' and finally the systems terminate in the A-type sesquioxide at O/M = 1,50, which is stable at high temperature.

viii) In the vertical direction of the diagrams the C'phase should terminate at low temperatures at the isotherm defined by the C→A transition temperature of the sesquioxide. This behaviour is established for the Pu-O system and can be expected also for the Pr-O and Ce-O systems on the basis of the data available though this has not yet been proved directly.

Therefore it would be interesting to prove or disprove this hypothesis for the systems Ce-O and Pr-O. Usually the high temperature A type phase seems to be more stable than the low temperature C-type phase. Furthermore it seems quite possible that the transformation C⟶A is always associated with a slight change in stoichiometry, see for instance [10] Pr-O, and [12] Pu-O. Also in the latter system it is not possible to prepare the C-form directly because the transformation temperature is too low. In the case of Ce_2O_3 the transformation temperature for C⟶A presumably also is too low to get the cubic C-form and in the case of Tb_2O_3 a tranformation to the B-form could be expected, but certainly only under very special conditions as can be deduced from [21]. For Pu_2O_3 the transformation temperature is T ≈ 350° C and for Pr_2O_3 it is T ≈ 850° C.

Generally speaking, one can divide each system into the four regions given in table I. The region where the Pu-O diagram clearly diverges from the common behaviour of the rare earth diagrams, is 1,83 ≥ O/M ≥ 1,70. In this range of compositions no intermediate stable phase is found in the Pu-O system, whereas two (Tb-O), three (Ce-O) or even four or five phases (Pr-O) exist for the rare earth oxides. These intermediate phases have all one important property in common, they have a distorted fluorite structure deficient in oxygen. Secondly they are stable only at lower temperatures, but the dissociation temperatures increase systematically with decreasing O/M-ratio.

This brief outline has shown that there are important properties in common for the oxide systems mentioned and that the region of divergence between the Pu-O and the rare earth systems is confined mainly to the low temperature part of 1,83 = O/M = 1,70. This will be further analysed in the next section.

Some authors, see for instance [13], classify the different suboxides in the rare earth oxide systems between 1,5 ≤ O/M ≤ 2,00 according to the formula :

(1) $MO_m = M_nO_{2(n-1)}$ $\quad n \geq 4$, integer

It is then proposed that those compositions obeying eq. (1) should be ordered structures and a model for the ordering process has been found [21]. Two important points in these phase diagrams cannot be explained by this formula : firstly why the first intermediate phase below MO_2 in all three rare earth oxide systems always appears near $O/M \lesssim 1{,}83$ and secondly why the bcc C'-type structure does exist invariably for $O/M \leq 1{,}69$ though the true bixbite C-type structure has $O/M \approx 1{,}50$. Surely arguments in addition to eq. (1) must be found in order to understand these oxide systems.

3. Lattice parameters of cubic and pseudo cubic phases

3.1. General behaviour

The available x-ray data at 20° C have been plotted in fig. 5 as cubic lattice parameters against O/M-ratio. The regions where the miscibility gaps occur in the phase diagrams at low temperature could be bridged somewhat by extrapolating data from the high temperature fluorite single phase to room temperature in the case of Pu-O and Ce-O, [3] [6]. In all cases for which distorted fluorite structures exist in the range $1{,}83 \geq O/M \geq 1{,}70$ (Pr-O, Ce-O, Tb-O) the pseudo cubic prameters have been employed in order to enable comparison with the true cubic phases. The division of the whole range $2{,}00 \geq O/M \geq 1{,}5$ into the four regions of table I is indicated in fig. 5. Unfortunately hardly any system has been investigated well enough for a complete analysis. For this reason we shall discuss only regions 1 and 3 of table I in some detail.

From fig. 5 we can state that for the three rare earth systems all cubic and pseudocubic lattice parameters between MO_2 and $MO_{1,69}$ are lying on a straight line solely with the exception of the $PrO_{1,71}$ and $CeO_{1,72}$ phases. The Tb-O system still keeps approximately to this behaviour. Beyond $MO_{1,69}$ there is a distinct break in the slope in the Ce-O system and the same seems to be true for the Pr-O system though more lattice parameters of the C'-phase are needed for this system. The Pu-O system behaves different but again beyond O/M = 1,69 the slope is changed and has a value very similar to that of the Ce-O system.

3.2. The region $2{,}00 \geq O/M \geq 1{,}83$ and its lattice parameters.

This region of compositions deserves special attention because here the development of the anion defect structure on a statistical basis starts. The investigation of

physical properties as function of defect concentration should give interesting results. Unfortunately such experiments have not yet been performed.

The slopes of the straight lines a = a (x) of figure 5 in the first region are given in table II. The values da/dx of the three rare earth oxides are practically the same in the region $2 \geq O/M > 1{,}72$ but the Pu-O system behaves different.

From fig. 5 and table II we see that in the Pu-O system at O/M = 2,00 the slope da/dx has a somewhat lower value than the rare earth oxydes and that it decreases further with decreasing O/Pu-ratio in the regions 1 and 2, (see table I).
This can also be seen from fig. 6 where the high temperature x-ray data of [12] for Pu-O and of [3] for Ce-O at 700° C are plotted in order to avoid extrapolation errors. The Pu-O system exhibits clearly a flatter slope than the rare earth oxides and we shall now analyse this in more detail.

Looking at the fluorite lattice as composed of spheres which are in contact with each other allows to write down the following relation between the ionic radii of the anions R_a and cations R_c and the lattice parameter a

$$(2) \quad R_c^{(4)} = \frac{\sqrt{3}}{4} a - R_a^{(-2)} \quad ; \; R_a^{-2} = \frac{a}{4}$$

With the lattice parameter known, R_c and R_a can be calculated, see table III, columns 5 and 6. Comparing these values with the values of column 2 shows that, according to equation (2) R_c is calculated about 5 % too large and R_a 3,7 % too small, if one takes $R_a = 1{,}40$ Å.

On the other hand the bond length

$$(3) \quad d = R_c^{(4)} + R_a^{(-2)}$$

is given about correctly, see columns 7 and 8 of table III. This behaviour indicates a distortion of the anions in the fluorite oxide structure i) an elongation in the direction of the bond anion-cation and ii) a contraction in the direction of the bond anion-anion. In the CaF_2 lattice this is not the case. The reason why in this discussion the ionic radii of Ahrens [25] see table III columns 2 and 3, have been used together with the radius R_a = 1,40 Å of Pauling and Zachariasen for O^{--} is the following :

If one constructs the fluorite lattice with the radii of column 2 table III, the big oxygen ions must be compressed somewhat in the direction O^{-2} - O^{-2} and have to be elongated a little in the direction M^{+3} - O^{-2}. This invalidates the stability criterium for the fluorite structure $R_{cation} : R_{anion} \geq 0{,}732$ [18] which is based on the Goldschmidt ionic crystal radii. In fact all corresponding ratios in column 4 of table III have $R_{cation} : R_{anion} < 0{,}732$ contrary to this rule with the exception of CaF_2. But that is exactly what one has to expect for the oxide fluorite structures. The large polarizing electric field of the M^{+4} ions certainly deforms the softer O^{-2} anions in the manner described.

The question if the trivalent radii of column 3 in table III can also be regarded as reliable in this context, is more involved since no direct comparison with lattice parameters is possible.

In the A-type rare earth structure (La_2O_3) the coordination number of the M^{+3} ions is 7 with three different distances [19], in PuO_2O_3 (hex) two different distances 2,36 Å and 2,62 Å for Pu^{+3} and its 7 next oxygen neighbours have been reported [20]. Therefore no reasonable radius of M^{+3} can be defined from these structures.

In the C-type rare earth structure on the other hand the M^{+3} ion has the coordination number 6 and all six bond lengths should be approximately equal, but the oxygen ions are not arranged in cubic symmetry around the cation.

Since this structure is very "open" one must expect some relaxation of the cation positions towards the empty tetrahedral positions, thus reducing the lattice dimensions. Therefore the lattice parameter cannot give any more an indication of the true radius of the M^{+3} cations also in this case.

We shall therefore proceed in a different way and we shall find that also the trivalent ionic radii given in table III column 3 should have approximately the correct size (possibly they are a little too large). This will be done by regarding the change of lattice parameter with the concentration of M^{+3} ions present. If x anions are removed at random from the MO_2 lattice, a lattice expansion results due to the corresponding change of z = 2 x cations from the state $R^{(+4)}$ to $R^{(+3)}$.

In table III the ionic radii $R^{(4)}$ and $R^{(3)}$ are given in columns 2 and 3. In each case the relative difference in R

$$(4) \qquad \frac{R_c^{(+3)} - R_c^{(+4)}}{R_c^{(+4)}} = \frac{\delta}{f} \approx 15\ \%$$

amounts to about 15 %. This is an extremely large misfit for two different atomic species on the same crystal lattice. From this fact it is clear that all phase diagrams discussed here show a miscibility gap at 20° C for $O/M < 2{,}00$.

For the relationship between a and x we may write from (2)

$$(5) \qquad a\,(z) = a_o + \frac{4}{\sqrt{3}}\, R_c^{(+4)} . z . \delta$$

$$(5a) \qquad z = 2\,x$$

The quantity δ is defined by eq. (4) and f is a factor which can be determined from the following equation (6)

$$(6) \qquad \frac{da}{dx} = \frac{8}{\sqrt{3}} \; f \; \Delta R$$

$$\text{with } \Delta R = R_c^{+3} - R_c^{+4}$$

by using the values of da/dx of table II and the values of R_c of table III. The values of f calculated in this manner are also listed in table II. The quantity f introduced here is a complicated function which could in principle be calculated from a detailed defect lattice model. This model would have to take into account the elastic expansion of the lattice due to the big M^{+3} ions at the one hand and the changes in the polarization and the relaxation of cation positions towards the center of each anion vacancy on the other hand. From eq. (6) we see that for f = 1 no relaxation exists but with $f < 1$ a relaxation and shift of ion positions is indicated which reduces the lattice expansion.

Two important facts can be drawn from the f-values in table II.

i) For the Ce-oxides we have for instance f = 0,77 this means 23 % of the radius difference ΔR is lost by relaxation effects of the lattice. Even if we would accept only 10 % as reasonable value for this effect, this would not change drastically the radii given in column 3 of table III. Therefore we can regard also these trivalent crystal radii as useful for our problem.

ii) If we compare the behavior of the rare earths with plutonium, the f-values of table II indicate a much more pronounced relaxation in the Pu-O system than with the rare earth oxides. Furthermore f remains constant in the latter systems up to the beginning of C'-type structure at $O/M \approx 1,69$ whereas it decreases continuously in the Pu-O system as far as f = 0,26 at O/Pu = 1,75.

This different behaviour of f for the Pu-O and the rare earth systems hints to the cause why no intermediate phases with a distorted fluorite structure are encountered in the Pu-O system.
The rare earth oxide lattice undergoes a constant rate of expansion when the oxygen content is decreased from O/M = 2,00 to 1,69. The result is an increasing field of internal stresses accompanied by an increase of free space in the structure. This must give rise to a cooperation shift of cation lattice positions if for some other reason the distribution of the stress centers (complexes of one anion vacancy with two M^{+3} ions) is changed.
The result is the distorted fluorite structures encountered in the rare earth oxide systems due to ordering of the anion vacancies as revealed by x-ray analysis.

The plutonium oxides on the other hand undergo a diminishing rate of expansion when decreasing the amount of oxygen in the lattice between O/M = 2,00 and 1,69 and therefore the field of internal stresses never attains a value which could give rise to cooperative phenomena. The basis of these differences between rare earth and Pu-oxides must lie certainly in the finer details of the homöopolar contribution to the crystal bonds, i.e. in the properties of the 4 f and 5 f states of the electron shells of rare earths and Pu.

3.3. Low oxygen boundary of the miscibility gap in the rare earth systems and some aspects of defect interaction in the region $1{,}83 \gtrsim O/M \lesssim 1{,}71$

In the rare earth oxide systems the first intermediate phase with distorted fluorite structure exists always in the vicinity $1{,}81 \lesssim O/M \lesssim 1{,}83$. This phase represents the low oxygen limit of the two phase regions under the

miscibility gap. We shall now inspect this limit more closely.

Each anion lattice site is the center of a tetrahedron whose four corners are occupied by cations. Since these are all equivalent, any two of them may change from the state + IV to + III if the center anion is removed. As long as we want to be sure of random distribution of the anion defects in MO_{2-x} we must require that the mean distance $d^{\langle hhl \rangle}$ between neighbouring anion vacancies in the main lattice directions is such that the corresponding cation tetrahedras do not share any corners or faces. Inspection of the fluorite lattice gives as minimum possible distances $d^{\langle hhl \rangle}$ under these conditions

$$(7) \qquad \begin{aligned} d^{\langle 111 \rangle} &= \frac{1}{2}\sqrt{3}\, a \\ d^{\langle 100 \rangle} &= a \\ d^{\langle 110 \rangle} &= \sqrt{2}\, a \end{aligned}$$

Taking into account the multiplicity of these lattice directions we get on purely geometrical grounds as average mean distance $\bar{d}$ of anion vacancies in the fluorite structure which does avoid ordering

$$\bar{d} \geq 1{,}15\ a.$$

From this the number of oxygen vacancies per unit cell is

$$\frac{1}{\bar{d}^3} \leq \frac{0{,}657}{a^3}$$

and this yelds

$$(8) \qquad \frac{O}{M} \geq \frac{2\,(8-0{,}657)}{8} = 1{,}832$$

By eq. (8) we have fixed the limiting composition in MO_{2-x} above which all vacancies may be distributed at random.

For $O/M < 1{,}832$ the anion vacancies must be partially or wholly ordered.

The arguments leading to equation (8) have only taken account of the geometry of the ideal lattice but not of the elastic interactions between the strain fields around the big trivalent ions. Presently nothing is known on the detailed structure of these defect complexes and therefore it is difficult to estimate their interaction from first principles. But since in the rare earth oxides both thermal expansion and expansion due to anion defects are linear functions, we may safely conclude that the lattice strain introduced by the defects can be compensated by thermal expansion. Disregarding second order effects like the increase of the coefficient of thermal expansion by lattice strain, we have the relation

$$(9) \qquad \frac{da}{dx} = \gamma \cdot \frac{da}{dT}$$

If an extra lattice strain is introduced, the ordering of vacancies gives rise to a distorted cubic structure. Now it is possible, according to eq. (9), to reduce this lattice strain by a certain amount of thermal expansion in such a way that the anion order may persist without extra strain, then this ordered structure is strainfree and cannot be detected anymore by x-ray methods.
From these arguments it follows that the temperature of dissociation, that is the peritectic temperatures of the intermediate distorted fluorite structures in the range $1{,}83 \gtrsim O/M \gtrsim 1{,}71$, should be related to the composition roughly via eq. (9). Replacing there the differentials by differences we get

$$10) \qquad \Delta T = \gamma \Delta x$$

where γ can be calculated from eq. (9) with $\frac{da}{dx}$ and $\frac{da}{dT}$ as determined by experiment, see table II. If we accept in the Ce-O system 450° C as temperature of dissociation

of the intermediate phase at $CeO_{1,81}$ we get as peritectic temperatures 670° C for $CeO_{1,78}$ and 1110° C for $CeO_{1,72}$ from eq. (10). This compares rather well with the temperatures to be found in fig. 2. For the Pr-O system no thermal expansion data seem to exist in the literature but again the same trend can be noticed in fig. 4, the intermediate non cubic phases have increasing peritectic temperatures with decreasing O/M ratio as to be expected from the equivalence of lattice expansion due to the elastic strain introduced by the M^{+3} ions with thermal lattice expansion. Of course the absolute stability of these phases can only be found by thermodynamic considerations.

The main conclusion from this qualitative model implies that at higher temperatures an ordered structure of anion vacancies also exists for $1,83 \gtrsim O/M \gtrsim 1,71$, but that the lattice is sufficiently strainfree to allow for the cation sublattice the symmetry of the true fluorite structure. The order of the anion vacancies might in principle be detected in x-ray diffraction patterns as superstructure lines. But the small atomic scattering factor of oxygen and the large half widths of the lines due to the high temperature will hardly allow to reveal these superstructure lines, but neutron diffraction should give useful results. The same arguments apply to the Pu-O system with the sole difference that also at lower temperatures, $T \doteq 650°$ C, the interaction between the defects is too weak due to the lattice relaxation and therefore no intermediate phases with distorted fluorite structure are realised at all, but still a degree of order must persist with respect to the anion vacancies because of the arguments which led to eq. (8).

3.4. The C'type phase $O/M \leq 1,69$

The fact that at $O/M \leq 1,69$ a new structure appears in the phase diagram, the C'-type-phase, is clearly seen in Fig. 5 and 6. The slopes of all (x) curves have a break at this composition and most important, the differences

between the structures of PuO_{2-x} and the corresponding rare earth oxides in the region $1{,}83 \gtrsim O/M \gtrsim 1{,}71$ do no more exist. Therefore a new structural principle common to all four oxide systems must work now.

In order to understand this new phase, we have to start from the other end of the phase diagrams from the stoichiometric C-type structure. It is, like the stoichiometric MO_2, a completely ordered phase. In the case of MO_2 we have created disorder by removing oxygen to get MO_{2-x}, now in the case of M_2O_3 we create disorder by introducing oxygen to get the C'-type phase. Since the C-type phase is common to all four sesquioxides discussed here, it is reasonable that also the C'-type phase starts at the same composition $O/M = 1{,}69$ for all four systems, since in all cases the same structural principles must be involved.

Recently Mulford has given a very clear discussion of the bcc M_2O_3 C-type structure [14]. It has a unit cell with the double cell edge of MO_2 and 16 oxygen ions removed in a regular manner, that is, two from each original MO_2 subcell. Thus the new bcc unit cell contains 32 cations. 48 anions and 16 ordered anion vacancies. As pointed out by Mulford, the bcc symmetry of this structure can only be retained if any extra oxygen atoms in the unit cell are distributed statistically on the positions of these 16 vacancies. In the Pu-O system Mulford looked for a composition of the C'-phase in the vicinity of $O/M \sim 1{,}61$ and found that 4 extra atoms per unit cell would give $O/M = 1{,}625$, thus $n = 4$. In the meantime this O/M ratio has in fact been found to a good approximation as the lower limit of the C'-phase in the Pu-O system [7]. From the figures 1,2 and 4 we know on the other hand that the upper limit of C' in all four phase diagrams is about $O/M = 1{,}69$; hence we have

$$\frac{48 + n}{32} = 1{,}69$$

or $n = 6$ for the upper phase boundary of the C'-phase. The lower limit in oxygen content for C' in the Ce-O system obviously is about $O/M = 1{,}65$ or $n = 5$. Thus we may have a generating formula for the limits of the domain of existence of the C'-phase similar to eq. (1)

$$(9)\quad MO_y\ ;\ y = \frac{48 + n}{32}\ ;\ n \leqq 6$$

In remains to be shown why $n = 6$ is the upper limit for the stability of the bcc C'-type structure.

4. Partial free enthalphy data in Pu-O and Ce-O systems and some relations with the phase diagrams.

4.1. The partial molar quantities of the Ce-O and the Pu-O system.

Both for the Ce-O [2] and for the Pu-O [15] systems data of the partial molar free enthalphy with considerable precision exist which can be compared and confronted with the results of the two previous sections. Since the scale in the representation of the EMF-data for the Pu-O system was rather small in the first publication [15] these data have been redrawn in fig. 7 on the basis of the originally measured points [6] represented as $\overline{\Delta G}$ versus temperature with the O/Pu-ratio as parameter. Furthermore the partial molar free entropies and enthalpies have been derived from the original curves [6] and have been refined in such a way that the whole set of data of fig. 7 can be recalculated by the relation (10) with reasonable error

$$(10)\quad \overline{\Delta G} = \overline{\Delta H} - T\ \overline{\Delta S}$$

with $\overline{\Delta H}$ and $\overline{\Delta S}$ independent of temperature. The results are compiled in table IV. $\overline{\Delta S}$ is plotted against O/M in fig. 8 together with the corresponding values of the

Ce-O system [2] . The latter data had to be multiplied by a factor 2 in order to have the same entropy scale as the one used in the EMF results on Pu-O.

The values $\overline{\Delta H}$ and $\overline{\Delta S}$ for the Pu-O system in table IV differ somewhat from the ones given by Rand [16] . These differences are not important for the integration of the partial molar properties in order to get integral thermodynamic chemical data as in the case of [16] , but they become interesting for the correlation of the partial molar quantities whith the details of the phase diagram. In the figures 1 and 2 the temperature regions of the phase diagrams covered by the investigation with the EMF method for Pu-O [6] and covered by the oxygen dissociation pressure method for Ce-O [2] are indicated by hatched areas.

4.2. Comparison of partial molar free enthalpy data with the Pu-O phase diagram and lattice parameters.

The Ce-O phase diagram as shown in fig. 2 has in fact been constructed on the basis of the partial molar free enthalpy data [2] , therefore nothing has to be added in this respect. The case of the Pu-O phase diagram is different. The $\overline{\Delta G}$-data first published [15] were correlated with the phase diagram of Gardner et al. [12] and agreement was assumed. When afterwards this phase diagram had to be modified on the basis of new experimental evidences [7] , the question arose if the $\overline{\Delta G}$ -data would also be in agreement with the modified phase diagram or if contradictions would exist. Therefore the re-evaluation of the EMF data as described in section 4.1. was undertaken.

Fig. 7 shows clearly two single phase regions at $2{,}00 \geq O/M \gtrsim 1{,}74$ and $1{,}67 \geq O/M \geq 1{,}63$. At 727° C and $1{,}90 \gtrsim O/M \gtrsim 1{,}80$ one recognizes already the miscibility

gap which will start to exist at little lower temperatures. The two single phase regions correspond exactly to i), the large single phase region PuO_{2-x} and ii) the C'-type phase in fig. 1. The latter phase shows only a relatively small change in $\overline{\Delta G}$ over its domain of existance, the limits O/Pu = 1,69 and 1,62 as established by [7] are not well defined in fig. 7 because of lack of experimental points. The most interesting region of fig. 7 is however $1{,}74 \geq O/Pu \geq 1{,}67$ which unfortunately does not show any experimental points. And this is probably the reason why this two-phase region escaped the attention of the authors who made the measurements.

If one extrapolates the curves from both sides of this experimental gap somewhat, as has been done in fig. 7 by the dotted lines, one sees that the $\overline{\Delta G}$ -curves on both sides of an area around $O/Pu \sim 1{,}70$ have different slopes. This difference is hardly observable at 727° C but it becomes more pronounced with increasing temperature. This is exactly the behaviour of curves which contain a short horizontal part whose length increases with rising temperature. In fact, these curves suggest a narrow two phase region around $O/Pu \sim 1{,}70$ which becomes larger with rising temperature.

The high temperature x-ray data given in fig. 6 correspond also with this interpretation, they show an irregularity in the same region of O/Pu-ratios. Therefore the two phase region C' + PuO_{2-x} has been drawn in fig. 1 around $O/M \sim 1{,}70$. From the point of view of the discussion on the lattice parameters and structures in the Pu/O system, this two phase region appears very natural and is satisfactory because it separates two structures, PuO_{2-x} and the C'-type structure which are developed from very different origins according to very different principles though with little difference in the two limiting compositions. This fact is also reflected by the behavior of $\overline{\Delta G}$ in fig. 7 and $\overline{\Delta S}$ in fig. 8 both for Ce-O and Pu-O. Both quantities show a drastic variation in the region $2{,}00 \geq O/M > 1{,}7$, but remain nearly constant for $1{,}69 \geq O/M \geq 1{,}6$. Thus in

all 4 systems of oxygen with Pu, Ce, Pr and Tb the composition O/M$\sim$1,70 divides each system in two different parts with very different properties.
Finally an interesting observation by [7] on quenched samples investigated at 20° C should be mentioned. Striking changes in the morphology of two phase structures have been found by metallography for samples with 1,70< O/Pu$\leq$ 1,995 as function of O/Pu-ratio. This behaviour is not yet investigated in detail. For the change of the morphology in the two phases between a sample with O/Pu= 1,78 and a sample with O/Pu = 1,80 however a correlation could be found with some changes in the x-ray properties at O/Pu$\sim$1,79. For O/Pu$>$ 1,79 the lattice parameter of the fluorite phase $PuO_{1,995}$ shows little scatter and the diffraction patterns give lines with very little line broadening. For O/Pu $<$1,79 on the other side the x-ray lines are very broad and the fluorite lattice parameter shows greater scatter. Since at O/M = 1,78 all rare earth oxide systems show an intermediate phase it is tempting to relate the observations in the Pu-O system at O/Pu$\sim$1,78 + 1,80 to some faint traces of an ordering process which cannot lead to a stable intermediate phase as in the rare earth oxides, but which presents itself as a change in transformation behaviour.

A look at the partial molar entropies $\overline{\Delta S}$ of Pu-O and Ce-O in fig. 8 is instructive in this connection.
In the Ce-O system the low temperature intermediate phases at O/Ce = 1,82 and 1,78 are revealed as superposed relative minima in the curves $\overline{\Delta S}$ versus O/Ce even for the entropies measured at temperatures above the peritectic temperatures of these phases. This is exactly what one must expect on the ground of the arguments put forward in section 3.3. In the Pu-O system on the other hand no such phases exist in a stable form, but still an indication of order, that is a flat relative minimum, is superposed on the basic $\overline{\Delta S}$ versus O/Pu-curve as can be

clearly seen by the break in the slope at O/Pu = 1,95 and in the following change of curvature for O/Pu < 1,95. From this curve one would rather expect the center of this minimum at O/Pu ~ 1,83 instead of O/Pu ~ 1,79 as indicated by the combined metallographic and x-ray results.

At the present state of experimental evidence any further conclusions would be purely speculative.

References

[1]	D.J.M. Bevan	J. inorg. nuc. chem. 1 49 (1955)
[2]	D.J.M. Bevan, J. Kordis	J. inorg. nuc. chem. 26 1509 (1964)
[3]	G. Brauer, K.A. Gingerich	J. inorg. nuc. chem. 16 87 (1960)
[4]	G. Brauer, H. Gradinger	Z. anorg. allg. chem. 277 89 (1954)
[5]	L. Eyring, N.C. Baenziger	J. appl. phys. Supl. I, 33 428 (1962)
[6]	T.L. Markin, R.J. Bones, E.R. Gardner - see also T.L. Markin	AERE - R 4724 (1964) Paper submitted to panel on thermodynamic properties of plutonium oxides. IAEA, Vienna, Oct. 1966. This paper contains some corrections on data published in ref. [12], below.
[7]	C. Sari, U. Benedict, H. Blank	EUR 3564 e (1967)
[8]	E.D. Guth, L. Eyring	J. am. chem. soc. 76 5242 (1954)
[9]	N.C. Baenziger et al.	J. am. chem. soc. 83 2219 (1961)
[10]	D.S. Chapin, M.C. Finn J.M. Honig	Rare earth research III p. 607 Proc. of the fourth conf. on rare earth research. Gordon and Breach 1965

[11]	D. Guth et al.	J. am chem. soc. 76 5239 (1954)
[12]	E.R. Gardner, T.L. Markin, R.S. Street	J. inorg. nuc. chem. 27 541 (1965)
[13]	B.G. Hyde, L. Eyring	Rare earth research III p. 623 Proc. of the fourth conf. on rare earth research. Gordon and Breach 1965.
[14]	R.N.R. Mulford	Paper submitted to panel on thermodynamic properties of plutonium oxides. IAEA, Vienna, Oct. 1966.
[15]	See for instance T.L. Markin , M.H. Rand	Thermodynamics Vol. I p. 145 fig. 3 IAEA, Vienna 1966.
[16]	M.H. Rand	Atomic energy review Vol. 4, special issue N° 1, pag. 27 IEA, Vienna 1966.
[17]	T.D. Chikalla, C.E. McNeilly R.E. Skavdahl	HW - 74802 (1962)
[18]	W. Kleber see also L. Pauling,	Einführung in die Kristallographie Veb Verlag Technik, Berlin 1961 The nature of the chemical bond Cornell Univ. Press 1960
[19]	A.F. Wells	Structural inorg. chemistry 3 rd edition. Oxford 1962
[20]	Structure reports 16 222	(1952)
[21]	G. Brauer	Progress in science and technology of rare earth. Vol. 2 p. 312 Pergamon press. 1966.

[22] S. Darbezat J. Loriers — C.R. acad. sci. 234 1978 (1952)

[23] H. Bommer — Z. Anorg. chem. 241 273 (1939)

[24] R.S. Roth, S.J. Schneider — J. res. natl. bur. stand. A 64 309 (1960)

[25] L.H. Ahrens — Geochim. and Cosmochim. Acta 2 155 (1952)

Captions to figures

Fig. 1. Proposed low temperature part of the Pu-O system based on the work of C. Sari et al [7], E.R. Gardner at al [12] and on the discussion given in section 4.2. of this paper.

Fig. 2. The Ce-O system after Bevan and Kordis [2] and Brauer and Gingerich [3] .

Fig. 3. The Tb-O system after Hyde and Eyring [13]

Fig. 4. The Pr-O system after Hyde and Eyring [13] with inclusion of the work on the C $\rightarrow$ A transformation by Chapin et al [10]. The compositions of the phases from which the pseudo cubic lattice parameters in fig. 5 have been taken are indicated as heavy bars. According to [13] they belong to metastable states. The true equilibrium phases according to these authors are indicated as dotted lines in the range $1{,}75 < O/M \leq 1{,}83$. Yet this complication in the phase relations does not affect the relation between pseudo cubic lattice parameters and O/M-ratio.

Fig. 5. Relations between O/M ratio and pseudo cubic and cubic lattice parameters in the systems Ce-O, Pr-O, Pu-O and Tb-O, see table V.- Points in square brackets were found by extrapolating high temperature x-ray data from $T \gtrsim 650°$ C to 20° C. The straight line for Pu-O between O/Pu = 1,69 and 1,62 stems from a least square analysis of room temperature lattice parameters of [7] .
Note the large deviations from the straight lines for the points at about 1,72 in the Ce-O and Pr-O systems and in the break in the slopes at O/M=1,69. Such a break exists also for the Pu-O system.

Fig. 6. Lattice parameters of Pu-O and Ce-O at 700° C.
For the purpose of comparison the room temperature values of Pu-O of fig. 5 are also shown. Note the difference in slope for the C'type structure of the Pu-O system at 20° C and at 700°C.

Fig. 7. Plot $\overline{\Delta G}$ versus O/Pu of the EMF-measurements of Markin et al. [15] [6].

Fig. 8. Plot of $\overline{\Delta S}$ versus O/M for the systems Ce-O [2] and Pu-O. The $\overline{\Delta S}$ -values for Pu-O have been derived from the original curves $\overline{\Delta G}$ versus T of [6], see also table IV.

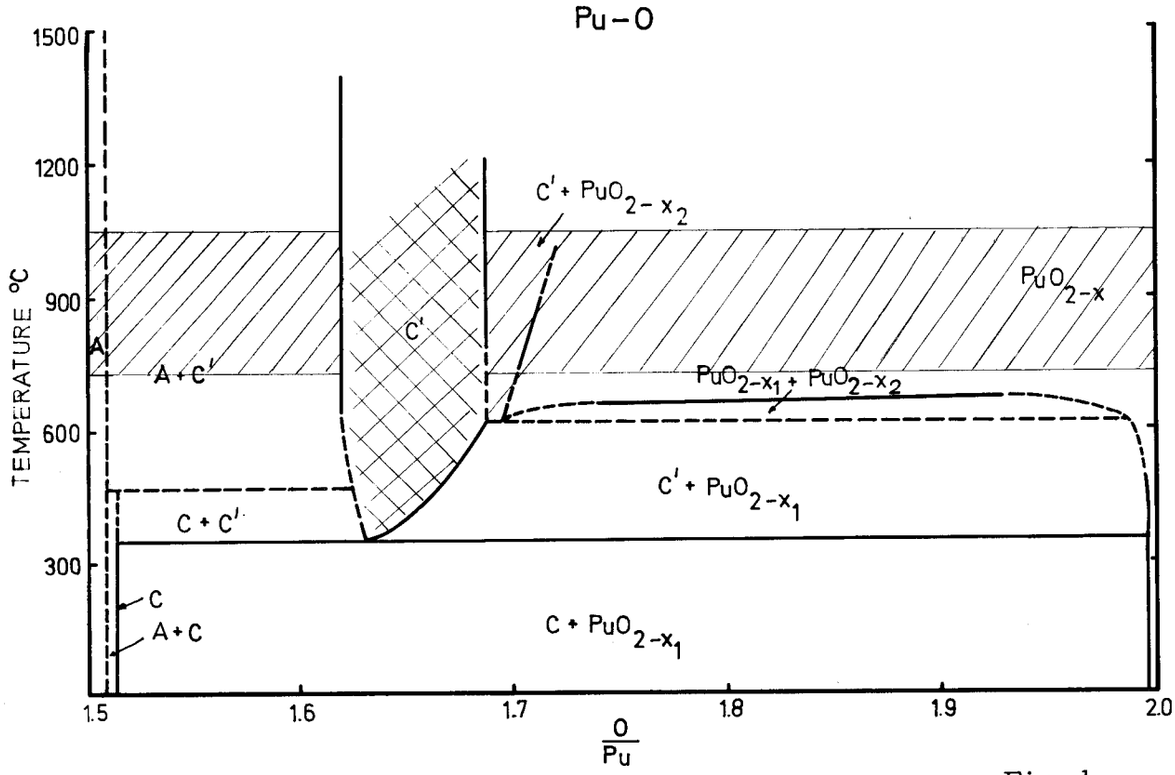
Pu – O
1500
1200
900
600
300
TEMPERATURE °C
A
A + C'
C'
C' + PuO2-x2
PuO2-x
PuO2-x1 + PuO2-x2
C' + PuO2-x1
C + C'
C
A + C
C + PuO2-x1
1.5
1.6
1.7
1.8
1.9
2.0
O/Pu

Fig. 1

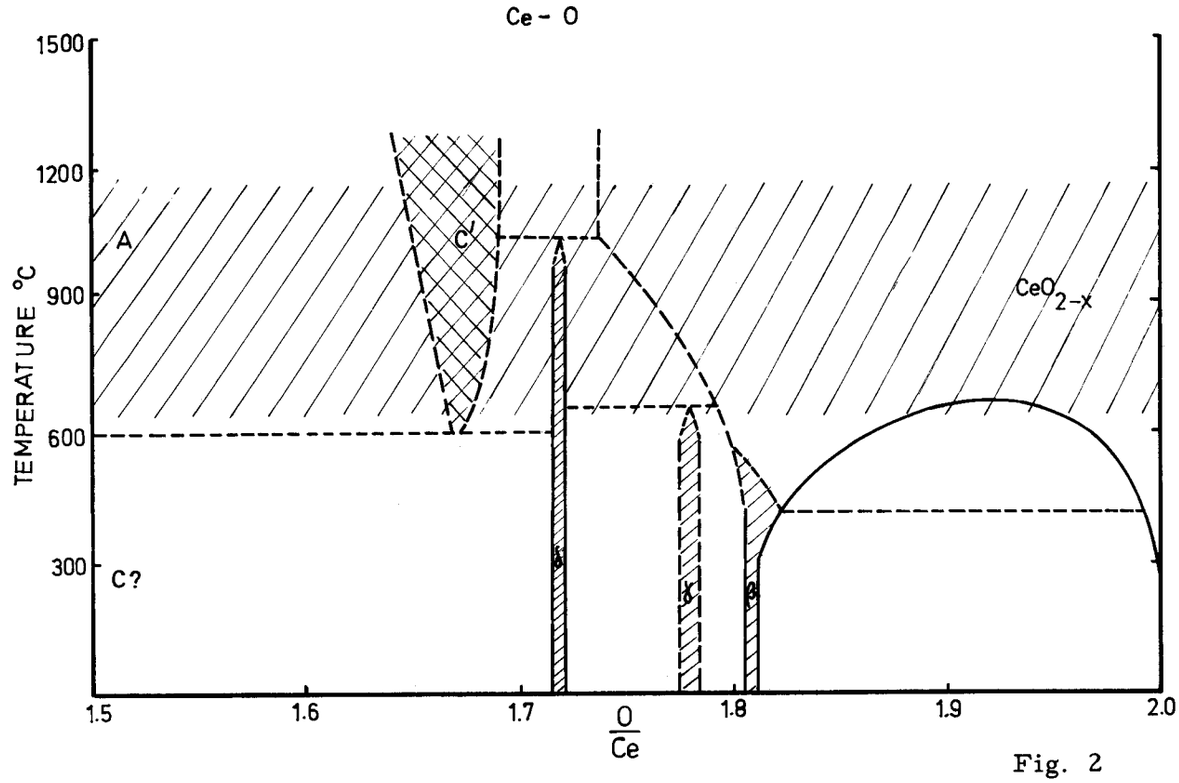
Ce – O
1500
1200
900
600
300
TEMPERATURE °C
A
C'
CeO2-x
C?
1.5
1.6
1.7
1.8
1.9
2.0
O/Ce

Fig. 2

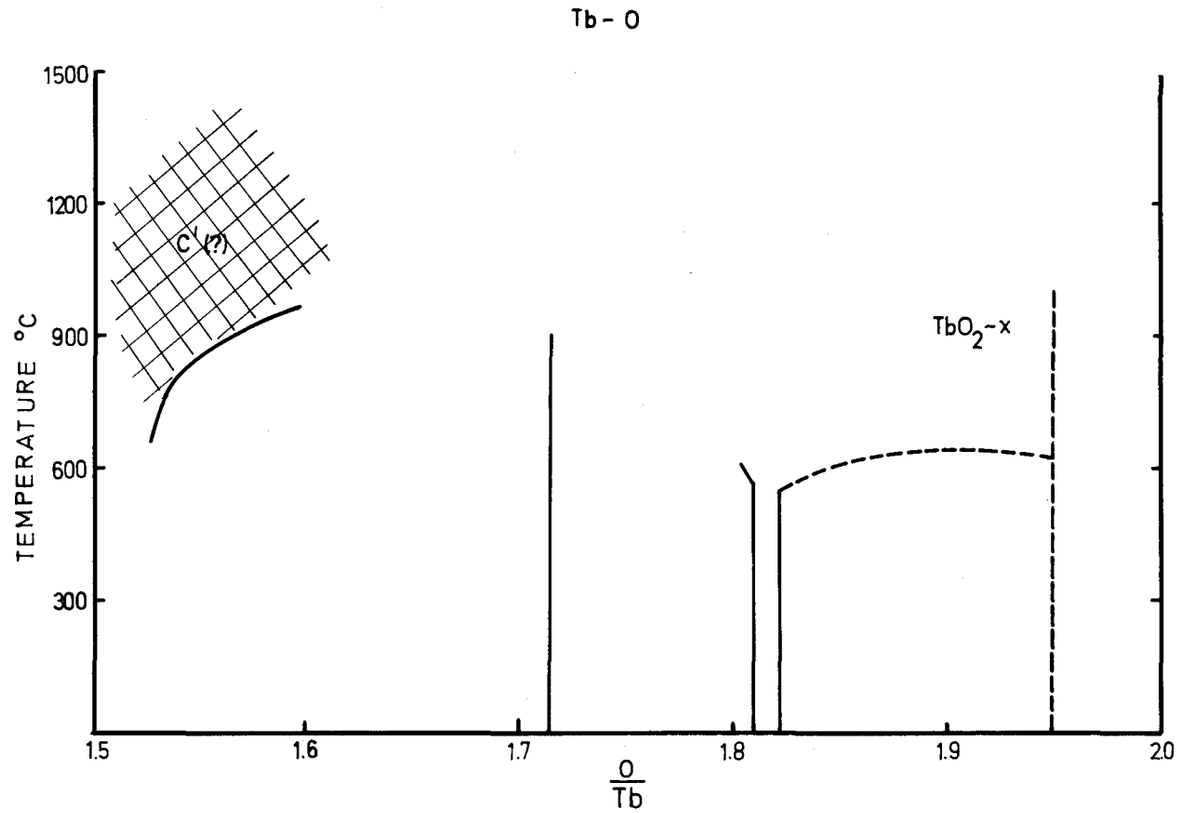
Tb - O
1500
1200
900
600
300
TEMPERATURE °C
C' (?)
TbO2-x
1.5
1.6
1.7
1.8
1.9
2.0
O/Tb

Fig. 3

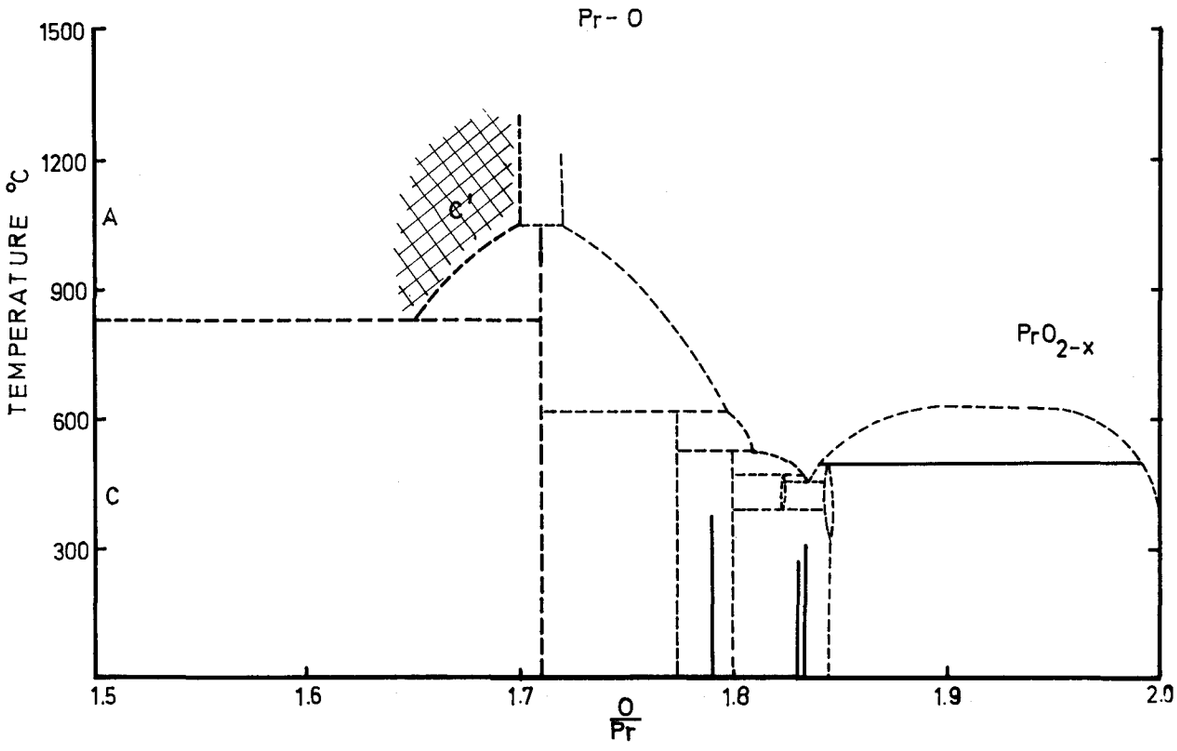
Pr - O
1500
1200
900
600
300
TEMPERATURE °C
A
C
C'
PrO2-x
1.5
1.6
1.7
1.8
1.9
2.0
O/Pr

Fig. 4

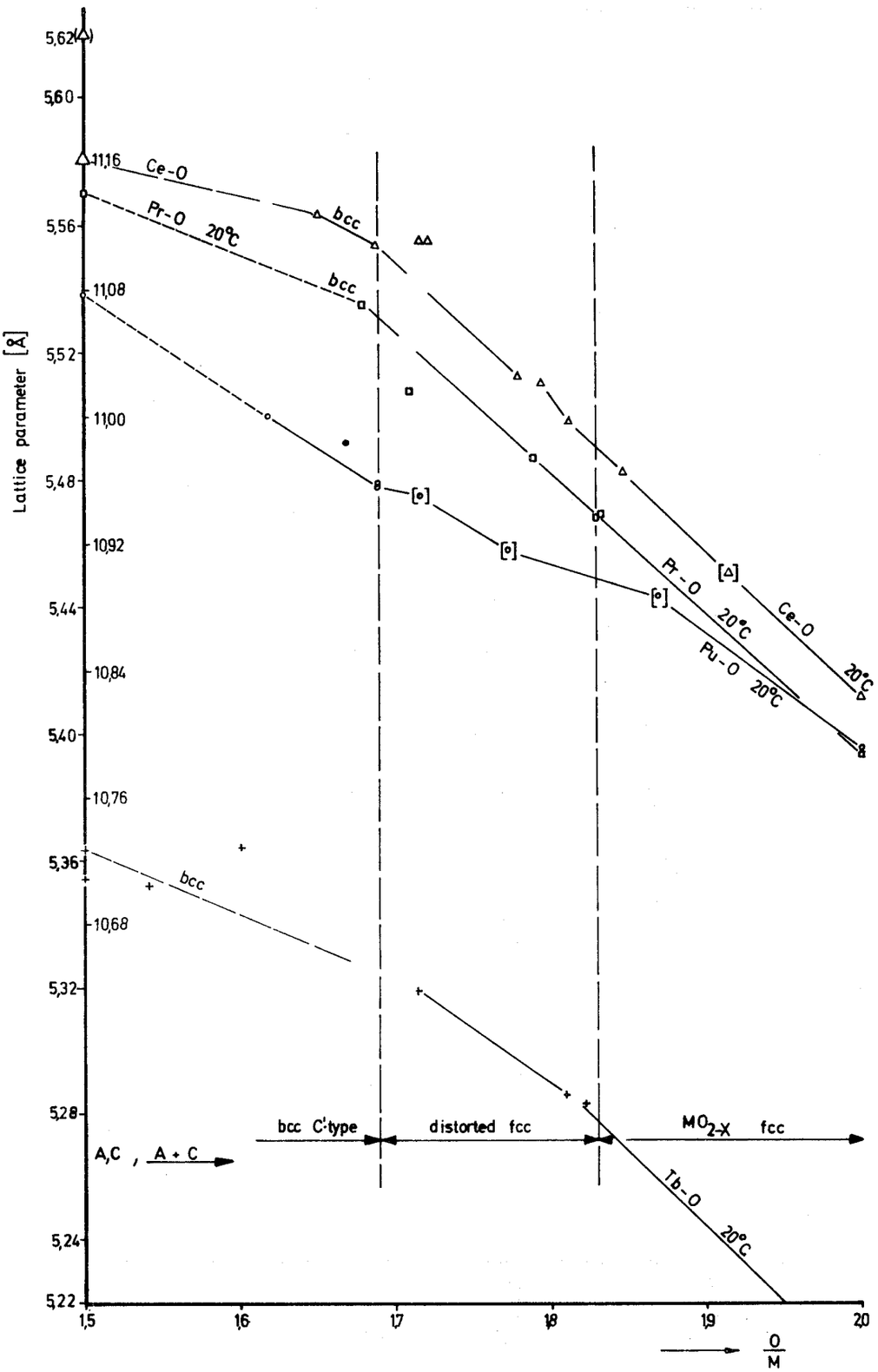
Lattice parameter [Å]
5,62
5,60
5,56
5,52
5,48
5,44
5,40
5,36
5,32
5,28
5,24
5,22
11,16
11,08
11,00
10,92
10,84
10,76
10,68
Ce-O
Pr-O 20°C
bcc
bcc
[o]
[o]
[o]
[Δ]
Pr-O 20°C
Ce-O 20°C
Pu-O 20°C
bcc
bcc C-type
distorted fcc
MO2-X fcc
A,C , A + C
Tb-O 20°C
1,5
1,6
1,7
1,8
1,9
2,0
O/M

Fig. 5

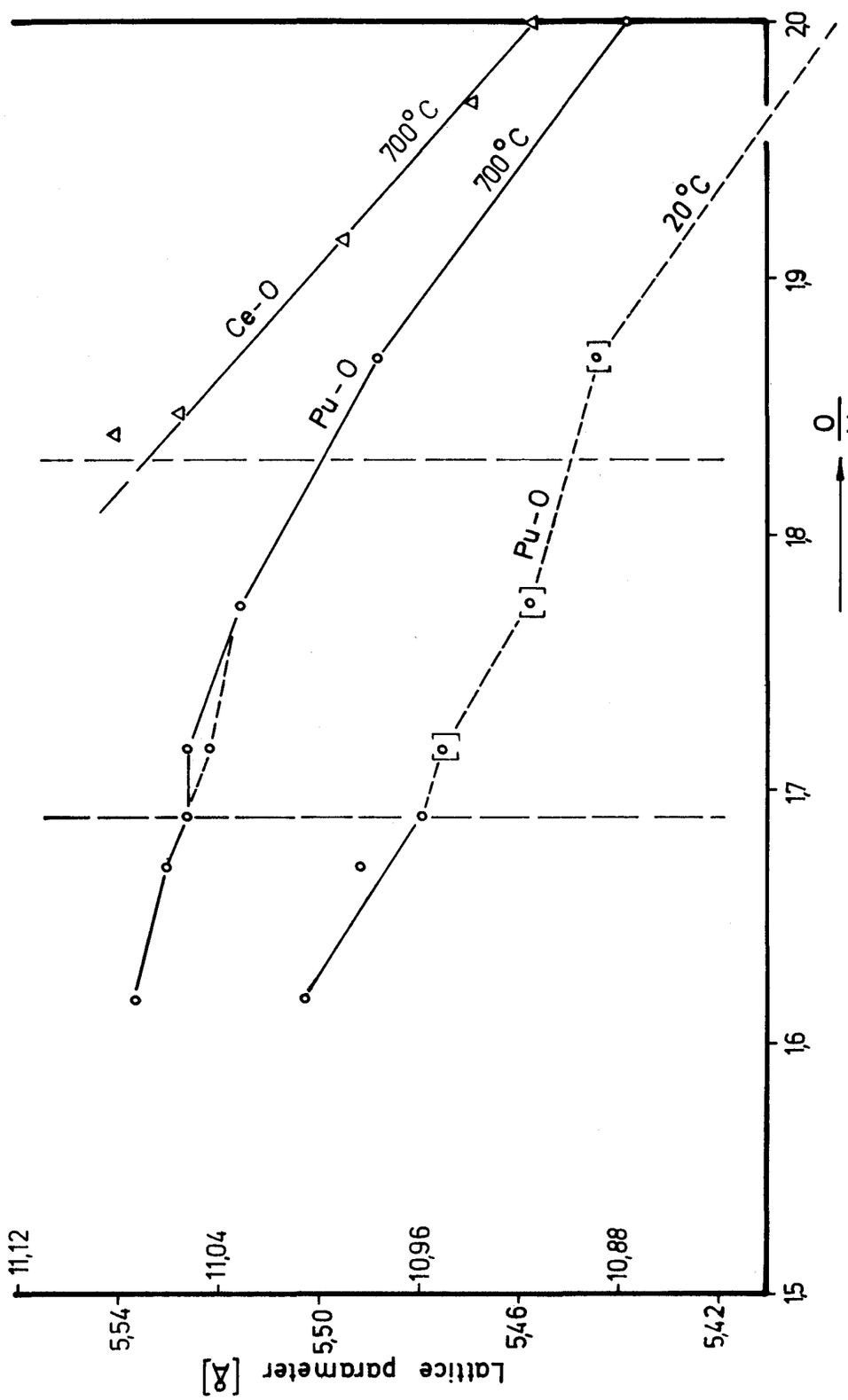
Lattice parameter [Å]
11,12
11,04
10,96
10,88
5,54
5,50
5,46
5,42
15
16
17
18
19
20
O/M
Ce-O
700°C
Pu-O
700°C
Pu-O
20°C
[°]
[°]
[°]

Fig. 6

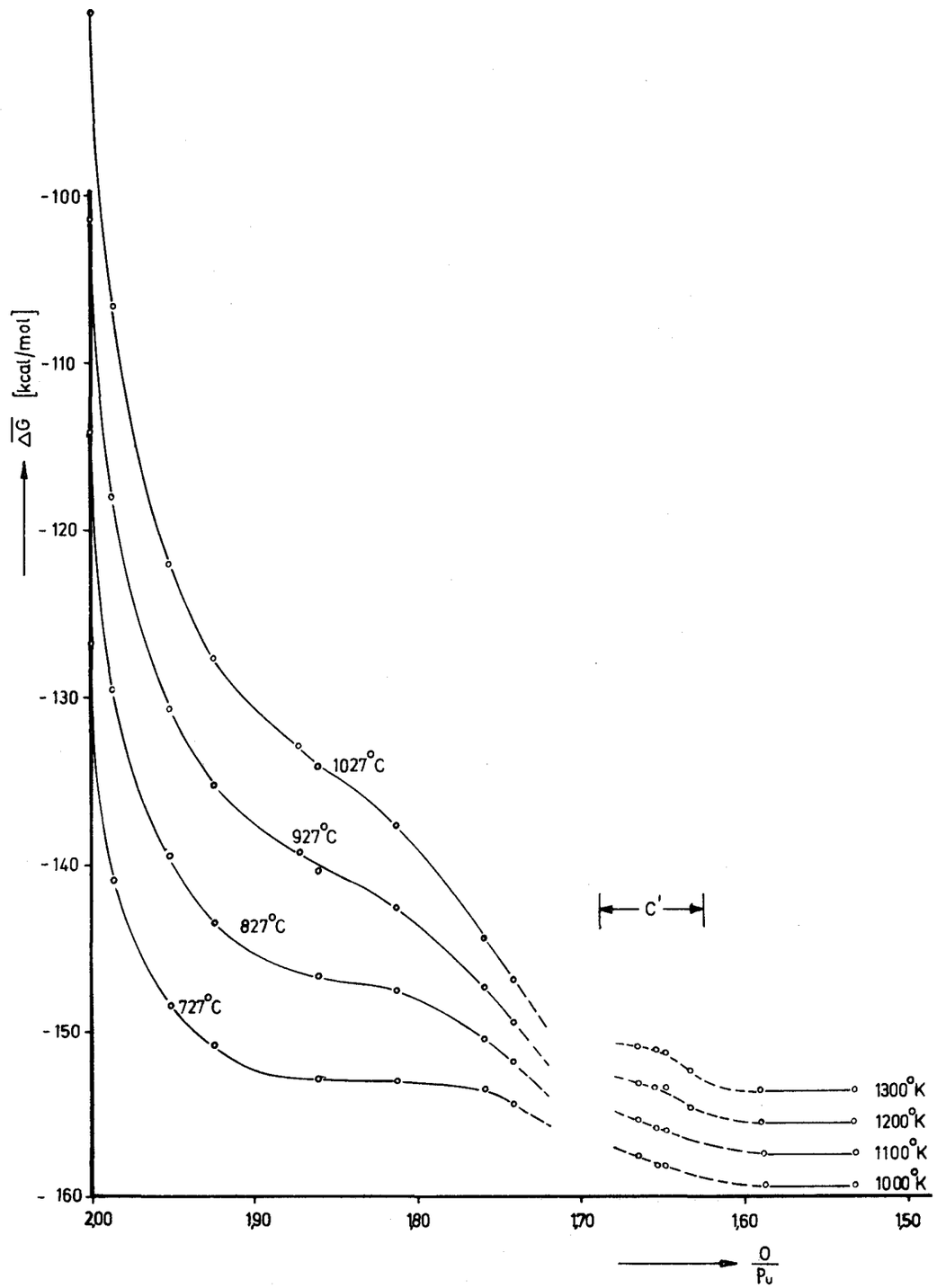
-100
-110
-120
-130
-140
-150
-160
$\overline{\Delta G}$ [kcal/mol]
1027°C
927°C
827°C
727°C
C'
1300°K
1200°K
1100°K
1000°K
2,00
1,90
1,80
1,70
1,60
1,50
O/Pu

Fig. 7

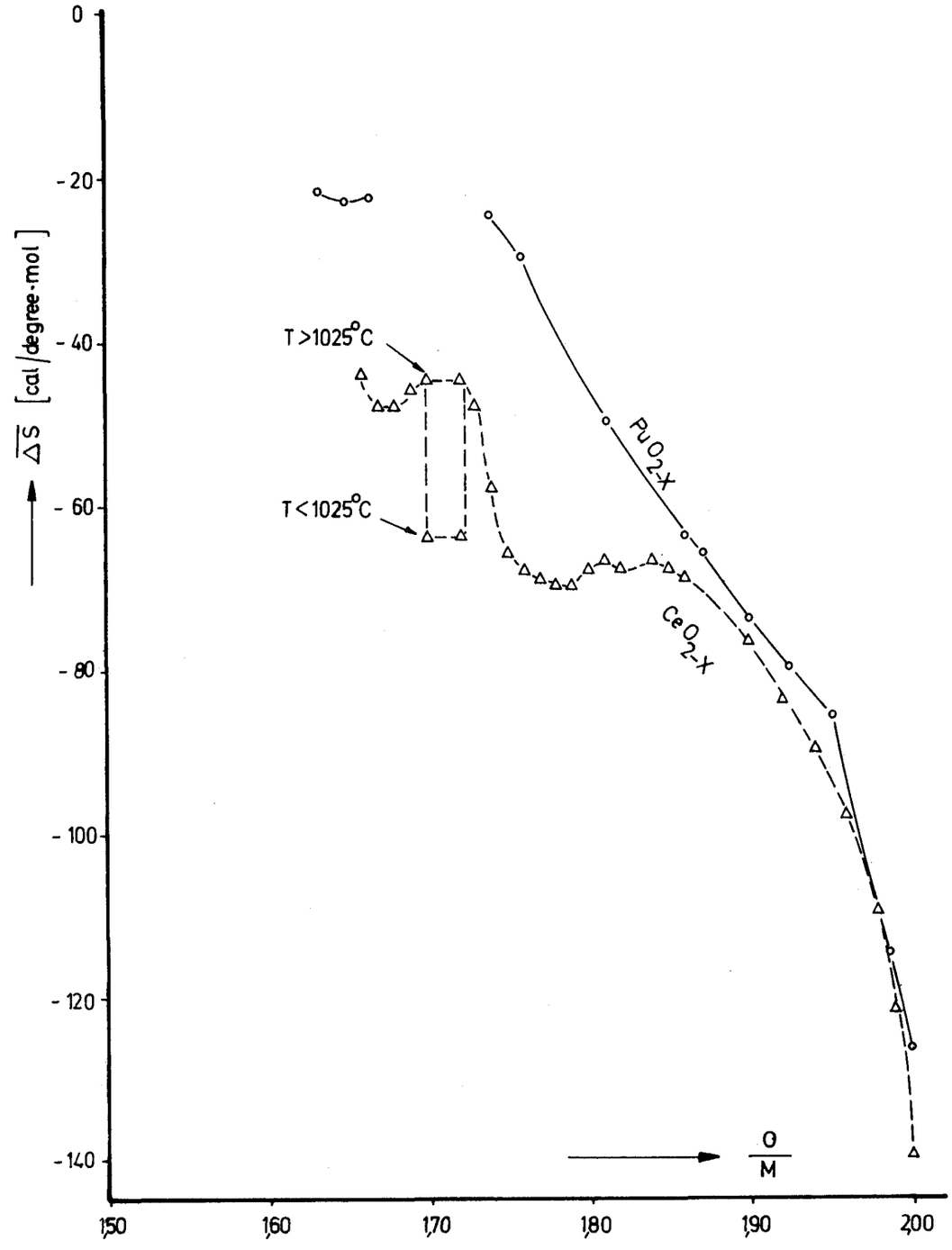
0
-20
-40
-60
-80
-100
-120
-140
$\overline{\Delta S}$ [cal/degree·mol]
T >1025°C
T <1025°C
PuO2-x
CeO2-x
O/M
1,50
1,60
1,70
1,80
1,90
2,00

Fig. 8

Table I

The division of the phase diagrams into four regions with different structural properties in the oxide systems of Pu, Ce, Pr and Tb.

Region	Range of O/M	Structure
1.	2,00 to 1,83	fcc fluorite defect structure, miscibility gap at $T < 650°$ C for rare earth and Pu.
2.	1,83 to 1,72	Distorted fluorite defect structures of non cubic symmetry for rare earth oxides.
3.	1,69 to Y *)	bcc C'-type structure for rare earth and Pu.
4. a)	Y*) to 1,50 $+\varepsilon$	C' + A two phase region or C type region
b)	1,50	depending on the tranformation temperature C $\longrightarrow$ A.

*) The composition Y may be 1,65 or 1,62, see section 3.4.

Table II

Variation of the cubic and pseudo cubic lattice parameters [1] with oxygen content and with temperature.

Oxide system	Ce-O		Pu - O					Pr - O		Tb - O
ΔR [Å]	0,13		0,15					0,14		0,12
Type of structure	pseudo-cubic + MO_{2-x}	C'	MO_{2-x}				C'	pseudo-cubic + MO_{2-x}	C'	pseudocubic + MO_{2-x}
Range of O/M	2,00-1,71	1,69-1,65	2,00-1,995	1,93	1,83	1,75	1,69-1,62	2,00-1,71	1,69-?	1,95 - 1,72
da/dx [Å]	0,465	~0,35	~0,4	0,385 [2]	0,284 [2]	0,18 [2]	0,314 [3]	0,447		0,48
f	0,775	0,582	~0,6	0,556	0,41	0,26	0,454	0,69		0,865
da/dT [Å/degr]	$0,631 \cdot 10^{-4}$ [5] $0,783 \cdot 10^{-4}$		$0,561 \cdot 10^{-4}$ [4]				$0,47 \cdot 10^{-4}$ [4]			
γ [degrees]	$0,736 \cdot 10^{4}$		$\sim 0,71 \cdot 10^{4}$				$967 \cdot 10^{4}$			

1) all lattice parameters have been expressed for the small fluorite unit cell
2) taken from measurements at 700° C [6] in order to avoid extrapolation errors
3) by least square analysis of data of [7]
4) taken from data of [6]
5) taken from data of [3], the second value of da/dT belongs to O/Ce = 1,84

Table III

Lattice parameters and ionic radii in the fluorite structure

	1	2	3	4	5	6	7	8
	a [Å]	R^{+4}	R^{+3}	R^{-2}/R^{+4}	$R^{-2} = \frac{a}{4}$	$R^{+4} = \frac{0,732a}{4}$	5 + 6	2 + R^{-2}
CaF_2	5,451	0,99	--	1,33 / 0,99	1,36	0,997	2,357	2,32
CeO_2	5,41	0,94	1,07	0,67	1,352	0,99	2,342	2,34
PrO_2	5,393	0,92	1,06	0,657	1,347	0,985	2,332	2,32
TbO_2		0,81	0,93	0,579				
ThO_2	5,59	1,02	--	0,729	1,398	1,022	2,420	2,42
UO_2	5,470	0,97	--	0,692	1,367	1,00	$2,367_5$	2,37
PuO_2	5,395	0,93	1,08	0,664	1,348	0,985	2,333	2,93

2) 3) Ionic radii due to Ahrens, see Kleber, Einf. i.d. Kristallographie

4) 8) The ionic radius of O^{--} has been taken 1,40 Å since this requires deformation of O^{--} in the fluorite structure, as to be expected by the large polarization. (Pauling-Zachariasen radius)

Table IV

$\overline{\Delta S}$ and $\overline{\Delta H}$ as evaluated from ref. [6] between 1000° K and 1300° K

O/Pu	$\overline{\Delta S}$ cal/degree	$\overline{\Delta H}$ Kcal/mol
1,633	21,7	180,7
1,65	23	181,3
1,665	22,5	180,2
(1,70)	--	--
1,741	24,8	179,2
(1,75)	(27,5)	(181,5)
1,759	30,0	183,5
(1,80)	(46,0)	(198)
1,812	50,0	202,7
(1,85)	(61,0)	(214)
1,86	64,0	217,3
1,871	66,0	218,8
(1,90)	(74,0)	(226)
1,924	80,0	231,7
1,951	86,0	233,8
1,986	115,0	256,1
2,00	127,0	254,0

The values of $\overline{\Delta S}$ and $\overline{\Delta H}$ for O/Pu = 1,75, 1,80, 1,85 and 1,90 have been taken from graphs of $\overline{\Delta S}$ and $\overline{\Delta H}$ versus O/Pu, therefore they are shown in brackets.

Table V/1

Ce - O

O/M	Phase	Cubic lattice const.	Rhomboedric or pseudo hexagonal lattice parameters		Reference
2,00	α	5,411	a	C	[1][3]
1,915	(α)	5,450	-	-	[3]
1,848	(α)	5,482	-	-	[3]
1,812 }	β	(5,497)	3,890	9,538	[1][4]
1,795 {		(5,510)	3,900	9,537	[1]
1,785 }	γ	(5,515)	3,91	9,502	[1]
1,775 {					
1,722 }	δ	(5,555)	3,912	9,657	[1]
1,717 {		(5,555)	3,921	9,637	[1]
1,688 }	C	11,107	-	-	[1]
1,651 {		11,126	-	-	[1]
1,50	C	11,24	-	-	[4]
		11,16	-	-	

tranformation temp: C $\longrightarrow$ A T $\sim$ 600° C (?)

The cubic parameters in brackets have been estimated from the pseudo hexagonal parameters of [1]

Lattice parameters at 710° C [3]

2,00	5,456
1,98	5,465
1,968	5,47
1,915	5,494
1,848	5,527

Table V/2

Pr - O

O/M	Cubic lattice parameter or fcr	Reference
2,00	5,393	[5]
1,833	5,469	[5]
1,830	5, 468 + extra lines	[5]
1,79	(5,487) α = 90° 7'	[5]
1,71	(5,508) α = 89.42'	[5]
1,68	11,070	[5]
1,50	11,140	[5]
	11,14	[23]

Transformation temp. C ⟶ A T ~ 800° + 850° C

Table V/3

Tb - O

$\frac{O}{M}$	Cubic or pseudocubic lattice parameter	Reference
2,00	-	
1,95	5,220	[9]
1,823	(5,285)	[9]
1, 810	(5,286)	[9]
1,715	(5,319)	[9]
1,601	10,728	
1,541	10,704	[8]
1,500	10,729	[8] [24]
1,500	10,728	[9]

Cubic parameters in brackets indicate true symmetry other than cubic.

Transformation temperature C $\longrightarrow$ B T < 750° C

Miscibility gap between $TbO_{1,71}$ and $TbO_{1,81}$ for T < 450° C

Table V/4

Pu - O

$\frac{O}{M}$	Cubic lattice parameters	Reference
2,00	5,395	[7]
1,870	[5,443]	[6]
1,773	[5,4575]	[6]
1,717	[5,475]	
1,69	[10,958]	[6]
1,69	10,95	[7]
1,62	11,01	[7]
1,618	(11,005)	[6]
1,51	11,058	[6]
1,50	11,08 *)	[7]

Cubic parameters in brackets are extrapolated to 20° C from high temperature x-ray data of [6]

*) Extrapolated from 1,09 + 1,62 to $\frac{O}{Pu}$ = 1,50

Tranformation temperature C → A T = 350° C

Lattice parameters at 700° C [6]

2,00	5,4375
1,87	5,4875
1,773	5,510
1,717	5,521 - 5,525
1,690	-
1,670	5,53
1,618	5,537

NOTICE TO THE READER

All Euratom reports are announced, as and when they are issued, in the monthly periodical **EURATOM INFORMATION,** edited by the Centre for Information and Documentation (CID). For subscription (1 year : US$ 15, £ 5.7) or free specimen copies please write to :

Handelsblatt GmbH
"Euratom Information"
Postfach 1102
D-4 Düsseldorf (Germany)

or

Office central de vente des publications
des Communautés européennes
2, Place de Metz
Luxembourg

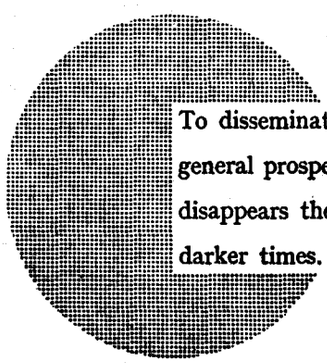

To disseminate knowledge is to disseminate prosperity — I mean general prosperity and not individual riches — and with prosperity disappears the greater part of the evil which is our heritage from darker times.

Alfred Nobel

SALES OFFICES

All Euratom reports are on sale at the offices listed below, at the prices given on the back of the front cover (when ordering, specify clearly the EUR number and the title of the report, which are shown on the front cover).

OFFICE CENTRAL DE VENTE DES PUBLICATIONS DES COMMUNAUTES EUROPEENNES
2, place de Metz, Luxembourg (Compte chèque postal N° 191-90)

BELGIQUE — BELGIË
MONITEUR BELGE
40-42, rue de Louvain - Bruxelles
BELGISCH STAATSBLAD
Leuvenseweg 40-42 - Brussel

DEUTSCHLAND
BUNDESANZEIGER
Postfach - Köln 1

FRANCE
SERVICE DE VENTE EN FRANCE DES PUBLICATIONS DES COMMUNAUTES EUROPEENNES
26, rue Desaix - Paris 15e

ITALIA
LIBRERIA DELLO STATO
Piazza G. Verdi, 10 - Roma

LUXEMBOURG
OFFICE CENTRAL DE VENTE DES PUBLICATIONS DES COMMUNAUTES EUROPEENNES
9, rue Goethe - Luxembourg

NEDERLAND
STAATSDRUKKERIJ
Christoffel Plantijnstraat - Den Haag

UNITED KINGDOM
H. M. STATIONERY OFFICE
P. O. Box 569 - London S.E.1

EURATOM — C.I.D.
51-53, rue Belliard
Bruxelles (Belgique)